

# International Journal of Engineering Sciences & Research Technology

(A Peer Reviewed Online Journal)  
Impact Factor: 5.164



**Chief Editor**

**Dr. J.B. Helonde**

**Executive Editor**

**Mr. Somil Mayur Shah**

**INTERNATIONAL JOURNAL OF ENGINEERING SCIENCES & RESEARCH  
TECHNOLOGY****SCINTILLATION EFFECT ON THE OF FREE SPACE OPTICAL  
COMMUNICATION IN SULAIMANI CITY / KURDISTAN REGION , IRAQ****Aras Saeed Mahmood**Department of Physics, College of Education, University of Sulaimani, Sulaimani, Kurdistan Region,  
Iraq

DOI: 10.5281/zenodo.7505813

**ABSTRACT**

Free Space Optical (FSO) communication systems is extremely dependent of the atmospheric weather conditions. The irregularities in the refractive index of the atmospheric layers created by the turbulent winds in the earth's atmosphere induces the optical turbulence which are responsible for random fluctuations in the signal carrying laser beam intensity (irradiance) called scintillations. The first objective of this study was to use the Hufnagel-Vally day with Sadot and Kopeika models together to calculate the refractive index structure parameter ( $C_n^2$ ) to estimate the strength of the scintillation in sulaimani city / kurdistan region, and it was found to be in the moderate to strong turbulence level. Secondly by utilizing the Optysystem-7 software, and due to the scintillation attenuation variation, the feasibility of the FSO communication in sulaimani city is found to be within the limit of about 5.5 km. Analyzing the BER, Max. Q factor, and the output power for the averaged months for five years from 2017-2021, it has been found that the best season for FSO communication is at the winter specially at January and the worst month is July of sulaimani summer.

**Keywords:** FSO communication, atmospheric turbulence, scintillation attenuation, and  $C_n^2$ **1. INTRODUCTION**

Free-space optics (FSO) refers to the transmission of modulated light pulses through free space (air or the atmosphere) to obtain broadband communications at speeds of up to 2.5 Gbps. This is not possible using any fixed wireless RF technology existing today. FSO technology requires no Federal Communications Commission (FCC) licensing or local license approvals and thus there is no need to buy expensive spectrum distinguishing from fixed wireless technologies [1]. This technology uses line of sight communication system and tries to achieve the need for high bandwidth over short distances [2 - 4]. There are numerous benefits of free space optics like no need for licensed frequency band allocation, easy to install, absence of radiation hazards of radio frequency, immunity to interference, high data rates [5 - 7], lower costs associated with the system, no fiber cable required, no rooftop installations, no digging roads is required and solves the last mile problem for fiber optics communication [8, 9]. In today's Internet community, demand of services consuming high data rates is increasing day by day. a lot of research is being carried out in the field of communication technology to fulfill high data rate demand with reliable quality of service and lowest cost possible. Lastly security is an important issue in between communication of two or more parties. by taking all these into consideration, Free Space Optics (FSO) is one of the choice to fulfill these demands [9 - 10].

However, local weather condition is the foremost limitation of FSO link availability and the feasibility of using FSO system as communication link very much depends on local weather [5, 11]. The atmosphere composition, weather and environmental factors like aerosol (small suspended particle), rain, snow, gases, fog, mist, and other different molecules interact with light propagation and directly affect the communication performance by attenuating the signal through scattering, absorption, and scintillation which results in a large path loss and limit the distance of the link [8, 12]. Molecular absorption attenuation results from an interaction between the radiation and molecules or atoms ( $N_2$ ,  $O_2$ ,  $H_2$ ,  $H_2O$ ,  $CO_2$ ,  $O_3$ , Ar, etc.) of the medium [3]. Atmospheric scattering (Aerosols scattering or Mie Scattering) occurs when the obstacle particle size are of the same order of magnitude as the wavelength of the transmitted wave, in optics it is mainly due to mist and fog, [4, 13]. There

[http:// www.ijesrt.com](http://www.ijesrt.com) © International Journal of Engineering Sciences & Research Technology

[9]



are a lot of researches on the above effects on the performance of FSO utilizing different models [4, 5, 9, and 14].

Even in clear day condition the gradient of pressure and temperature (nonhomogeneity) present in the atmosphere lead to what is known as atmospheric turbulence causing the index of refraction fluctuations for atmospheric layers. Using laser beam when signal propagate through such turbulent atmospheric layers, it will experience random fluctuations, and induces an extra spreading of the beam, i.e. the broadening of the beam size beyond of that expected due to pure diffraction [10]. The variations in the amplitude and phase of the received signal due to atmospheric turbulence effect are known as scintillation. Scintillation causes deep signal fading that lead to increase bit errors, i.e., when detection hardware does not receive adequate optical power and hence degrades the link performance especially for link ranges greater than 1km [8]. This phenomena contribute to the degradation of FSO performance, through the random fluctuations of the signal-carrying laser beam intensity (irradiance), and perhaps most important difference between Fiber Optics and FSO is that FSO is affected by prevailing conditions of environment.

## 2. ATMOSPHERIC TURBULENCE and SCINTILLATION

Optical turbulence occurs when turbulent winds in the earth's atmosphere mix the always-present vertical moisture and temperature gradients caused by the sun's heating of the earth's surface. This creates irregularities in the refractive index of the atmosphere in the form eddies, or cells, called optical tubules [12]. Optical turbulence is an important microphysical effect that acts on the propagation of light waves to distort optical propagation paths and intensity. Along the propagation path of a free space laser communication system, optical turbulence can produce significant intensity fluctuations and variations in the direction of the transmitting beam propagation [13]. The quantitative intensity measurement of optical turbulence is known as the refractive index structure parameter or constant ( $C_n^2$ ), having different ranges of  $10^{-16}$ ,  $10^{-15}$  and  $10^{-14}$  for weak, middle and strong turbulence respectively [12]. Considering the vertical path, the behavior of  $C_n^2$  is conditioned by temperature changes along the different layers within the Earth's atmosphere, hence, the refractive-index structure parameter becomes a function of the altitude above ground, i.e.  $C_n^2(h)$ . There are different models for predicting  $C_n^2(h)$  such as submarine laser communication (SLC), Hufnagel-Valley Day (HV), Hufnagel-Valley Night, Greenwood [10] and Hufnagel, Andrews and Phillips (HAP) model [13], however the most common and appropriate one is HV- day model which is the one used in this work and given as:

$$C_n^2(h) = 0.00594 \left(\frac{v}{27}\right)^2 (10^{-5}h)^{10} e^{(-h/1000)} + 2.7 \times 10^{-16} e^{(-h/1500)} + A e^{(-h/100)} \quad (1)$$

where  $h$  is in meters [m],  $v$  is the wind speed in meters per second [m/s], and  $A$ , is a nominal value of  $C_n^2$  ( $h=0$ ) at the ground and equals  $1.7 \times 10^{-14} \text{ m}^{-2/3}$ . Based entirely on macroscale meteorological parameters another scientific macroscale model is suggested for estimating  $C_n^2$  that includes additional parameters such as solar flux and total cross-sectional area (TCSA) of the aerosol particulates per cubic meter having a significant effect on beam scintillation known as Sadot and Kopeika model [10,13,15, 16] given by

$$C_n^2 = 5.9 \times 10^{-15} W_{th} + 1.6 \times 10^{-15} T - 3.7 \times 10^{-15} RH + 6.7 \times 10^{-17} RH^2 - 3.9 \times 10^{-19} RH^3 - 3.7 \times 10^{-15} WS + 1.3 \times 10^{-15} WS^2 - 8.2 \times 10^{-17} WS^3 + 2.8 \times 10^{-14} SF - 1.8 \times 10^{-14} TCSA + 1.4 \times 10^{-14} TCSA^2 - 3.9 \times 10^{-13} \quad (2)$$

For  $C_n^2$ , in units of  $\text{m}^{-2/3}$ . In Eq. (2),  $W_{th}$  is a temporal hour weight (0.1),  $T$  is temperature (kelvin);  $RH$  is relative humidity (%);  $WS$  is wind speed (m/s),  $SF$  is solar flux and equals  $1.37 \text{ kW/m}^2$ ,  $TCSA$  is total cross-sectional area of particles per cubic meter ( $\text{cm}^2/\text{m}^3$ ) and its approximate expression can be found in [10] as:

$$TCSA = 7.3 \times 10^{-3} + 9.96 \times 10^{-4} RH - 2.75 \times 10^{-5} RH^2 - 1.37 \times 10^{-5} SF^4 \quad (3)$$

The scintillation measurements in general may yield information about overall effective  $C_n^2$  rather than just refractive index structure parameter  $C_n^2(h)$  [13]. That is

$$C_n^2(\text{total}) = C_n^2(h) + C_n^2 \quad (4)$$

The first studies on the atmospheric turbulence effects on propagating light waves were conducted by Tatarskii (1971) using the Rytov method [10]. A laser beam propagating through the atmosphere will be altered by refractive-index inhomogeneity. At the receiver plane, a random pattern is produced both in time and space, The parameter that express these irradiance fluctuations is the scintillation index or the normalized Rytov variance ( $\sigma_1^2$ ). The weak fluctuations regime occurs when  $\sigma_1^2 < 1$ , and the strong fluctuations regime is associates with  $\sigma_1^2 > 1$  [10,12]. The relation between refractive index structure parameter  $C_n^2$  and the relative variance of optical intensity (scintillation variance)  $\sigma_1^2$  was set by Rytov as:

$$\sigma_1^2 = K C_n^2 k^{7/6} L^{11/6} \tag{5}$$

Where  $k$ , represent the wave number ( $2\pi/\lambda$ ), the wave length ( $\lambda$ ) in (nm),  $L$  is the distance between the transmitter and the receiver of the optical wireless in meters and  $K$  is a constant equal to 1.23 for plane wave and 0.5 for spherical wave [12].

Scintillation peak to peak amplitude is equal to  $4\sigma_1$  and attenuation related to scintillation is equal to  $2\sigma_1$  [3], the relation for the turbulence or scintillation attenuation  $\alpha_{scint}$  in dB (for spherical wave and for all turbulence regimes from weak to strong can be written as [17]:

$$\alpha_{scint} = 2 \sqrt{\left(0.5 C_n^2 \left(\frac{2\pi}{\lambda}\right)^{7/6} L^{11/6}\right)} \tag{6}$$

In this paper we calculate the strength of the  $C_n^2$  and then analyze the effect of the scintillation on the performance of FSO communication in the sulaimani city using the data from sulaimani metrological station. Optisystem-7 is utilized to perform simulative analysis.

### 3. METHODS and MATERIALS

This study presents the methods and materials for analyzing the scintillation phenomena and the feasibility of free space optical communication in sulaimani city using Hufnagel Vally (HV) day with Sadot and Kopeika models together. The study used quantitative data involved humidity, temperature, wind speed and altitude. The data was secondary data from sulaimani metrological station for monthly average of 60 months from 2017 to 2021 as shown in table 1.

**Table 1: Sulaimani Metrological Station Data**  
**Monthly Average Temperature (C°)**

Year	Jan	Feb	Mar	Apr	May	Jun	Jul	Aug	Sep	Oct	Nov	Des
2017	6.6	5.8	12.3	18.0	24.3	30.1	34.8	34.6	30.7	21.3	14.4	11.6
2018	8.0	10.3	16.0	18.2	22.6	29.8	33.7	33	29.5	22.0	13.7	09.0
2019	7.1	08.6	10.2	14.8	24.4	31.7	32.5	34.1	28.8	23.0	14.7	10.1
2020	6.9	07.7	13.6	17.6	24.6	29.8	34.7	32.2	31.1	24.5	15.7	10.3
2021	9.0	11.0	14.0	21.7	27.9	31.3	35.3	34.8	28.6	22.5	15.0	10.1

**Monthly Average Relative Humidity (%)**

Year	Jan	Feb	Mar	Apr	May	Jun	Jul	Aug	Sep	Oct	Nov	Des
2017	65.4	66.7	68.8	56.9	39.8	30.6	24.2	26.2	29.5	43.9	62.6	59.1
2018	65.8	70.1	57.1	55.2	52.8	30.3	26.8	30.4	33.2	51.4	71.8	82.5
2019	77.2	68.6	70.4	65.3	46.4	29.7	28.1	29.7	32.6	47.3	48.6	69.9
2020	73.0	70.0	62.9	59.7	41.4	28.1	25.7	28.1	29.0	33.6	64.9	67.7
2021	58.6	63.0	57.3	42.6	33.2	27.9	28.6	27.9	32.8	40.3	55.7	65.9

**Monthly Average Wind Speed (m/s)**

Year	Jan	Feb	Mar	Apr	May	Jun	Jul	Aug	Sep	Oct	Nov	Des
2017	0.8	0.9	1.3	0.1	0.1	0.1	0.2	0.1	0.1	0.7	0.6	0.6
2018	0.9	0.7	1.0	1.5	1.3	1.3	1.1	1.2	1.5	1.6	1.0	0.6
2019	0.8	1.2	1.6	1.3	1.5	1.7	1.5	1.9	1.5	1.1	1.1	1.0
2020	1.5	1.0	1.7	1.4	1.7	1.5	2.0	2.4	1.5	1.4	0.9	0.6
2021	1.5	1.4	1.4	1.3	1.7	1.6	1.9	1.8	1.2	1.1	1.3	0.9

#### 3.1. Studied Area



The study focused on the Sulaimani city which is one of the most famous cities of Kurdistan region and Iraq. It is located at the north east of Iraq ( Lat. 35.33 and Long. 45.27) with elevation or altitude ( $h$ ) of 884.8 meters above sea level. Sulaimani is a highly populated (779 thousand people over 20,144 km<sup>2</sup>), the requirement for higher and unlimited bandwidth is necessary day by day for getting high quality of communication network. To investigate the performance of the feasibility of using FSO communication in the above studied region, Optisystem-7 software has been used to simulate a proper proposed communication link (Fig.1).

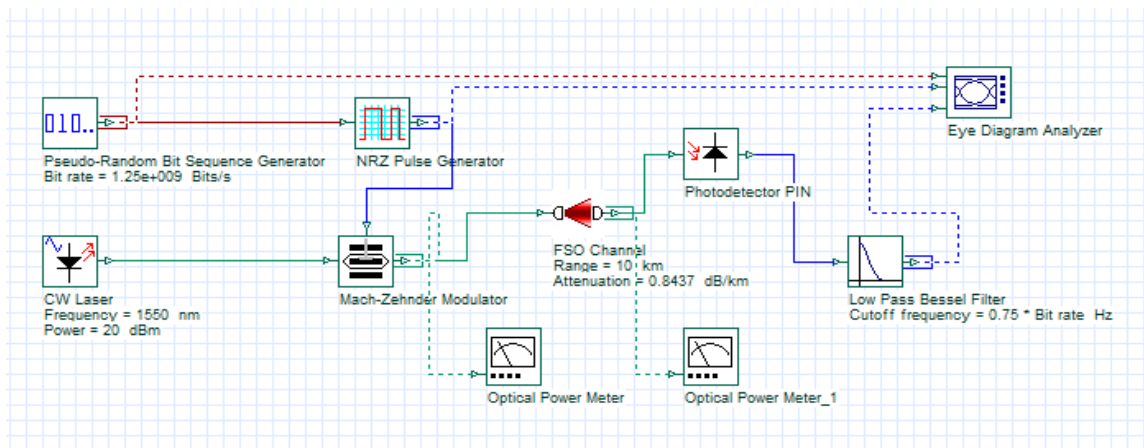


**Fig. 1: Block Diagram of FSO-NRZ System Simulation with Scintillation Effect**

### 3.2. Simulation Design

Optisystem-7 is an optical communication system simulation package to design, test and optimize any type of optical link. The simulation setup shown in fig.1, consists of three blocks which are transmitter, receiver and the propagation channel (atmosphere). The transmitter block comprises of Pseudo-Random bit sequence (PBRs) generator generates signal in the binary format converted into an electrical signal by NRZ pulse generator. Further, the optical signal produced by a continuous wave (CW) laser source having operating frequency corresponds to 1550 nm (atmospheric attenuation produces less effect at this frequency [18]) is modulated by Mach-Zehnder modulator with respect to electrical output produced by NRZ pulse generator. The modulated optical beam is transmitted through free space optic (FSO) channel block, which was set to 1-8 km, towards the receiver block.

The receiver block consists of a PIN photodetector and a low pass Bessel filter. The photodetector was used for optical to electrical conversion before signal flow to a low pass Bessel filter for further filter out any high frequency noise component present in the signal. The decoded signal will then arrive at signal inspection equipment such as BER analyzer or Eye-Diagram analyzer to compute eye diagram quality, minimum BER and Q-factor of the designated system, besides the received power was measured using Optical Power Meter. The designed parameters and their values are tabulated in the table 2 below.

**Table 2: Simulation Parameters**

Design Parameter	values
Operating Signal wavelength, $\lambda$	1550 nm
Link Rang, $L$	$1 \leq L \leq 8$ km
Receiver Aperture Diameter	20 cm
Transmitter Aperture Diameter	5 cm
Beam Divergence	2 mrad
Optical Power	20 dBm
Receiver Type	PIN
Cut off Frequency	7.5 GHz
Modulation Scheme	NRZ
Transmission Bit Rate	1.25 GBits/s

### 3.3. Scintillation Attenuation

Scintillation attenuation calculation in sulaimani city was performed using equation 6 with different link ranges from 1 to 8 km under Hufnagel-Vally (HV) day with Sadot and Copeika models together considering spherical wave propagation. To do that we have to calculate monthly average refractive index structure parameter  $C_n^2$ .

First, the average metrological data (Temperature, Relative Humidity and Wind speed) for the years from 2017 to 2021 was calculated from table 1 and tabulated in table 3 below.

**Table 3: Temperature, Relative Humidity and Wind speed Average  
Data for the Years from 2017 to 2021**

Month	Temperature (C°)	Relative Humidity (%)	Wind Speed (m/s)
January	7.52	68.00	1.10
February	8.68	67.68	1.04
March	13.22	63.30	1.40
April	18.06	55.94	1.12
May	24.67	42.72	1.26
June	30.54	29.68	1.24
July	34.20	26.68	1.34
August	33.74	28.46	1.48
September	29.74	31.42	1.16
October	22.66	43.30	1.18
November	14.70	60.72	0.98
December	10.10	69.02	0.74

Second, using all the values within the above table in the equations 1, 2, 3, and 4 separately, the monthly average refractive index structure parameter  $C_n^2$ (total) for the years 2017 to 2021 has been calculated as in the table 4 below.

**Table 4: Calculated the monthly average refractive index structure  
parameter  $C_n^2$  for the years 2017 to 2021**

Month	$C_n^2$ (m <sup>-3/2</sup> ) × 10 <sup>-14</sup>
January	2.1312
February	2.4922
March	4.0542
April	4.7272
May	5.6842
June	6.0972
July	7.9552
August	7.7252
September	6.8752
October	5.3492
November	4.7732
December	3.6852

The refractive index structure parameter  $C_n^2$  is related to the scintillation index through the equation 5, so for different link distance from 1 to 8 km, the monthly average scintillation index for the years 2017 to 2021 has been calculated and finally by utilizing the equation 6 with replacing  $C_n^2$  by  $C_n^2$ (total). The monthly average attenuation due to scintillation ( $\alpha_{scint}$ ) in dB, for link distance of 1 to 8 km for the years 2017 to 2021 in sulaimani region has been calculated and finally to use the attenuation in the software the attenuation in dB/km has been calculated and tabulated in table 5.

**Table 5: Scintillation attenuation ( $\alpha_{scint}$ ), in dB/km, monthly averaged for the years 2017 to 2021 per distance from 1 to 8 km.**

Month	1 km	2 km	3 km	4 km	5 km	6 km	7 km	8 km
January	0.7803	0.7357	0.7107	0.6936	0.6808	0.6701	0.6613	0.6539
February	0.8438	0.7966	0.7686	0.7500	0.7359	0.7246	0.7152	0.7071
March	1.0762	1.0146	0.9802	0.9555	0.9386	0.9242	0.9121	0.9018
April	1.1621	1.0956	1.0585	1.0330	1.0135	0.9979	0.9849	0.9738
May	1.2743	1.2014	1.1607	1.1327	1.1114	1.0943	1.0800	1.0679
June	1.3197	1.2443	1.2021	1.1731	1.1510	1.1334	1.1186	1.1060
July	1.5075	1.4213	1.3731	1.3399	1.3148	1.2946	1.2727	1.2632
August	1.4856	1.4006	1.3531	1.3205	1.2956	1.2757	1.2591	1.2449
September	1.4015	1.3213	1.2765	1.2557	1.2223	1.2035	1.1878	1.1744
October	1.2362	1.1655	1.1260	1.0988	1.0781	1.0616	1.0477	1.0360
November	1.1678	1.1009	1.0636	1.0379	1.0184	1.0025	0.9897	0.9786
December	1.0260	0.9674	0.9347	0.9120	0.8949	0.8811	0.8696	0.8598

#### 4. SIMULATION ANALYSIS

In this section, we discuss about the results observed from our proposed FSO design (Fig.1), using simulation parameters in Table 2. Under H-V day with Sadot and Copeika models together the simulation of the FSO link was attained under different ranges from 1 to 8 km with their corresponding attenuations in dB/km of table 5 over Sulaimani region from the year 2017 to 2021. The Q factor and the minimum bit error rate (BER) recorded from the eye diagram analyzer presented in table 6 and 7 respectively.

**Table 6: The Calculated maximum Q factor**

Month	1 km	2 km	3 km	4 km	5 km	6 km	7 km	8 km
January	730.80	181.14	71.33	34.92	20.01	12.16	7.76	3.5
February	721.70	176.32	68.56	33.28	18.80	11.28	7.10	4.64
March	689.15	160.05	59.33	27.91	14.96	8.55	5.14	3.20
April	677.45	154.38	56.23	26.09	13.72	7.71	4.56	2.79
May	662.43	147.27	52.43	23.90	12.27	6.74	3.89	2.32
June	656.44	144.48	50.96	23.06	11.73	6.38	3.66	2.15
July	632.15	133.48	45.31	19.88	9.71	5.08	2.81	0.00
August	634.94	134.72	45.94	20.22	9.92	5.22	2.88	0.00
September	645.76	139.59	48.42	21.43	10.80	5.78	3.25	0.00
October	667.50	149.65	53.69	24.63	12.75	7.05	4.10	2.47
November	676.68	154.02	56.04	25.98	13.65	7.66	4.52	2.76
December	696.07	163.45	61.20	28.98	15.71	9.08	5.51	3.47

**Table 7: Calculated minimum Bit Error Rate (BER)**

Month	1 km	2 km	3 km	4 km	5 km	6 km	7 km	8km
January	0.00	0.00	0.00	2.13E-267	2.33-E89	2.59E-34	4.33E-15	1.40E-7
February	0.00	0.00	0.00	3.95E-243	3.64E-79	8.4E-30	6.08E-13	1.70E-6
March	0.00	0.00	0.00	9.84E-172	8.28E-51	6.2E-18	1.38E-7	6.78E-4
April	0.00	0.00	0.00	2.43E-150	3.63E-43	6.13E-15	2.61E-6	2.65E-3
May	0.00	0.00	0.00	1.51E-126	6.52E-35	8.00E-12	5.03E-5	1.01E-2
June	0.00	0.00	0.00	5.61E-118	4.73E-32	8.96E-11	1.33E-4	1.56E-2
July	0.00	0.00	0.00	3.31E-088	1.40E-22	1.89E-7	2.45E-3	1
August	0.00	0.00	0.00	3.00E-091	1.62E-23	9.05E-8	1.99E-3	1
September	0.00	0.00	0.00	3.55E-102	1.69E-27	3.80E-9	5.80E-4	1
October	0.00	0.00	0.00	3.37E-134	1.61E-37	8.63E-13	2.03E-5	6.73E-3
November	0.00	0.00	0.00	4.45E-149	1.04E-42	9.02E-15	3.10E-6	2.87E-3
December	0.00	0.00	0.00	5.68E-185	6.69E-56	5.50E-20	1.77E-8	2.58E-4

The output power that is the optical power after the propagation and before the PIN photo detector at the receiver side of the link also recorded by an optical power meter and tabulated in the following table 8.

**Table 8: The output power of the system before the PIN photo diode**

Month	1 km $\times 10^{-6}W$	2 km $\times 10^{-6}W$	3 km $\times 10^{-6}W$	4 km $\times 10^{-6}W$	5 km $\times 10^{-6}W$	6 km $\times 10^{-6}W$	7 km $\times 10^{-6}W$	8 km $\times 10^{-6}W$
January	391.41	85.54	32.93	16.04	8.91	5.37	3.44	2.29
February	385.76	83.17	31.63	15.23	8.36	4.98	3.15	2.08
March	365.66	75.23	27.33	12.60	6.62	3.78	2.29	1.46
April	358.50	72.47	25.89	11.73	6.07	3.42	2.04	1.27
May	349.36	69.03	24.13	10.70	5.42	2.99	1.75	1.07
June	345.72	67.68	23.45	10.31	5.18	2.83	1.64	0.996
July	331.09	62.37	20.83	8.84	4.29	2.27	1.28	0.746
August	332.76	62.99	21.12	9.00	4.39	2.33	1.31	0.771
September	339.27	65.32	22.27	9.56	4.77	2.57	1.47	0.878
October	352.43	70.18	24.71	11.04	5.63	3.13	1.84	1.13
November	358.03	72.30	25.80	11.68	6.4	3.39	2.02	1.26
December	369.91	77.88	28.20	13.12	6.96	4.01	2.46	1.57

From the table 6, the values of the maximum Q- factor for the months July, August, and September corresponding to the 6 km link distance ( almost the longest accepted distance in this study) are 5.8, 5.22, and 5.78 which are all less than 6 (the minimum acceptable value for maximum Q- factor [19] ). Same thing is true for the BER values which were  $1.89 \times 10^{-7}$ ,  $9.05 \times 10^{-8}$ , and  $3.8 \times 10^{-9}$  (table 7) for the same months and link distance, all these values more than  $10^{-9}$  which is the standard maximum accepted value for FSO communication links which means that if we transmit  $10^9$  bit then only 1 bit have error. To get the more proper optimal link distance for feasibility of FSO in sulaimani city, the same previous calculation steps were repeated to calculate the monthly averaged scintillation attenuation for the link distance of 5.5 km. Table 9 shows the results of the eye diagram analyzer after simulation of the same proposed link.

**Table 9: Monthly averaged 5 years (from 2017 to 2021) Attenuation, maximum Q-Factor, BER, and output power for 5.5 km link distance.**

Months	Attenuation (dB/5.5 km)	Max. Q- Factor	BER	Output power ( $\times 10^{-6} W$ )
January	0.6750	15.49	2.08E-54	6.859
February	0.7299	14.46	1.09E-47	6.398
March	0.9310	11.23	1.53E-29	4.959
April	1.0053	10.22	8.41E-25	4.514
May	1.1024	09.03	8.75E-20	3.992
June	1.1418	08.58	4.54E-18	3.797
July	1.3042	06.97	1.57E-12	3.091
August	1.2852	07.14	4.54E-13	3.167
September	1.2124	07.84	2.19E-15	3.472
October	1.0694	09.42	2.35E-21	4.162
November	1.0102	10.15	1.61E-24	4.486
December	0.8876	11.86	9.69E-33	5.240

Figures 2 and 3 show the variation of the monthly averaged maximum Q- factor and the output power with the months for the optimum link distance (5.5 km) for FSO communication in Sulaimani respectively.



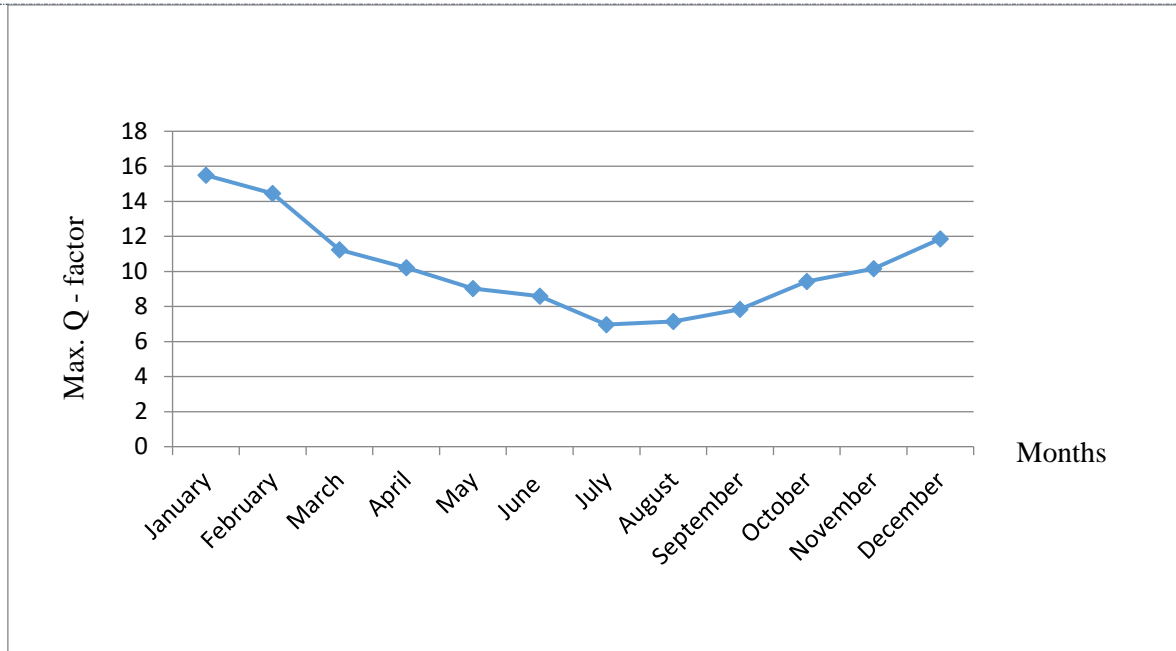


Fig. 2: Q - factor vs. months for 5.5 km link distance

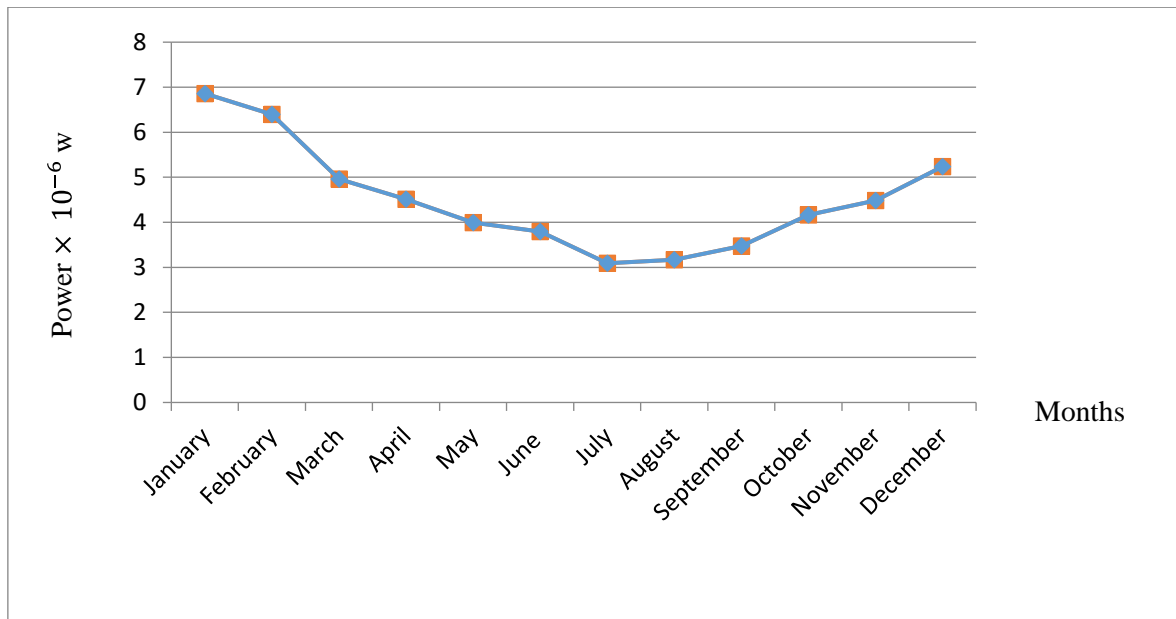


Fig. 3: Output power vs. months for 5.5 km link distance

The eye diagrams for the average monthly five years from 2017 to 2022 for the proposed link of fig.1 under 5.5 km link distance shown in figure 4 below.

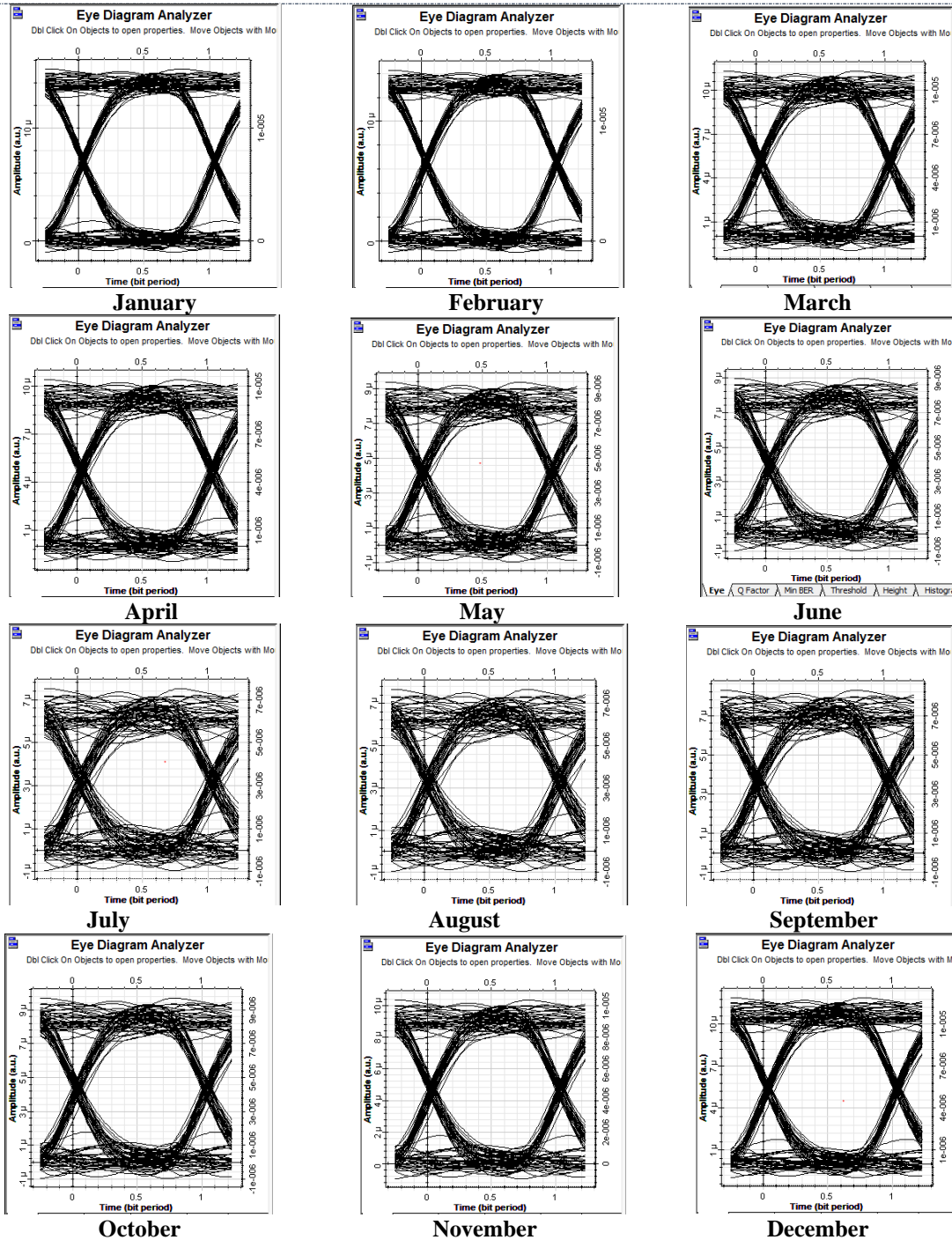


Fig. 4: Eye diagram for the average monthly five tears under 5.5 km link distance

5. RESULTS ANALYSIS

Calculation of the scintillation attenuation ( $\alpha_{scint}$ ), in dB/km, monthly averaged for the years 2017 to 2021 per distance from 1 to 8 km shown in table 5 presents that the attenuation due to scintillation in sulaimani varies with the months besides its decreasing value with increasing the link distance as shown in the figure 5. The lowest attenuation was 0.6539 dB/ km in January and the highest attenuation was 1.5075 dB/km in July as tabulated in table 5. These values corresponds to the minimum and maximum values of the refractive index structure parameter

( $2.1312 \times 10^{-14} \text{ m}^{-3/2}$  and  $7.9552 \times 10^{-14} \text{ m}^{-3/2}$ ) respectively presented in table 4.

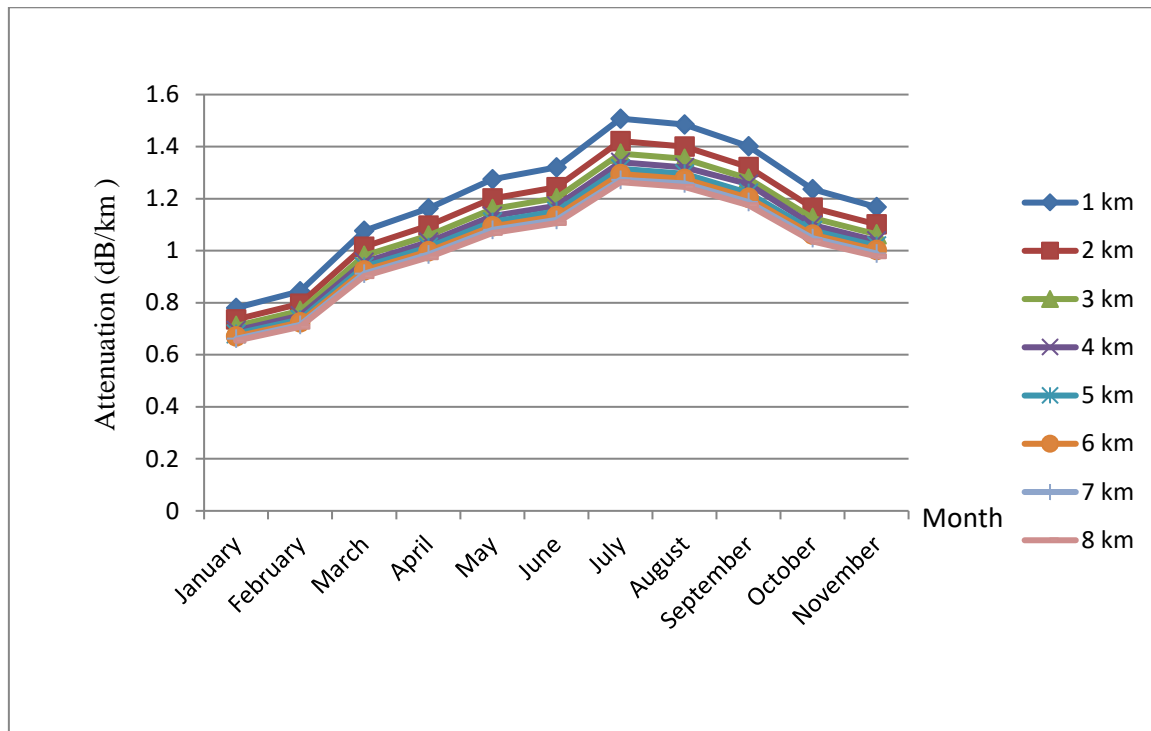


Fig. 5: Attenuation vs. months for different link distance

The availability of the FSO link in sulaimani further estimated from the values of the Q – factor given in table 6. The highest value was 730.8 in January and the lowest value was zero in the months July, August, and September. The Q – factor which decreases with the link distance has all accepted values up to 5 km link ( the minimum accepted value for Q - factor is 6) but for 6 km link and beyond there were some months having values less than 6. The Bit Error Rate denotes how much error occurs after communication in the bit sequence and its value for better communication is  $10^{-9}$ . Table 7 presents all the values for all the months in sulaimani for different link distances, and shows how it increases with the distance. The values are all accepted up to 5 km, while for 6 km and beyond there are some values which are more than  $10^{-9}$  and not accepted for good communication.

The output power of the system tabulated in table 8, gave the same indication about the impact of the monthly scintillation on the performance of the FSO communication in sulaimani, the highest output power was in January and the lowest in July for all different link distances. Those results encouraged to test the mid distance between 5 and 6 km, i.e. 5.5 km link distance which gave a very good and accepted monthly averaged Q – factor and BER over all the 60 months between 2017 to 2021 as shown in the table 9.

Figures 2 and 3 show, how the maximum Q – factor and the output power varies with averaged months for 5 years under the scintillation in sulaimani. The minimum output power and Q- factor appear in July, while there values increases toward the months December and January.

The eye opening of the eye diagram analyzer that gives the quality of the communication for the averaged months under 5.5 km link distance presented in figure 4, shows the variation of the quality of the FSO communication with the months. It is clear that in winter ( Dec., Jan., and Feb.) especially in January there is the best communication quality and the worse is in July ( summer).

## 6. CONCLUSIONS

At the end of the study the following points are concluded:

[http:// www.ijesrt.com](http://www.ijesrt.com) © International Journal of Engineering Sciences & Research Technology

- 1- The calculated values of the refractive index structure parameter ( $C_n^2$ ) for all the months, presented in table 4, and since they are all more than  $10^{-14}$ , indicates that the scintillation in sulaimai can be considered to be in the moderate to strong turbulence regime (level) [20].
- 2- Scintillation is one of the most atmospheric effects on the FSO communication in sulaimani because of the large difference in the temperature, Humidity, and wind speed between the months of the year.
- 3- The FSO system availability decreases with increasing the link of the propagation and the FSO communication is feasible in sulaimani for about 5.5 km range.
- 4- The best season for FSO communication in sulaimani is its local winter specially at January and the worst season is the summer specially in July.
- 5- The performance of this work is useful to see the feasibility and validity of FSO link usage for every country.

## 7. ACKNOWLEDGMENT

The author gratefully acknowledge Sulaimani Metrological Station for the support of the project and supplying all the data concerning the project.

## REFERENCES

1. Sadiku MNO, Musa SM, Nelatury S. "Free Space Optical Communications: An Overview" in European Scientific Journal February, 12(9):55-68, 2016
2. Ghoname S, Fayed HA, Aziz AAE, Aly MH. "Performance Analysis of FSO Communication System: Effects of Fog, Rain and Humidity" in Sixth International Conference on Digital Information Processing and Communications (ICDIPC) 21-23 April 2016. DOI: 10.1109/ICDIPC.2016.7470809. pp 151-155, 2016
3. Al Naboulsi M, Sizun H, de Fornel F. "Propagation of optical and infrared waves in the atmosphere" in Environmental Science, Physics. Retrieved from [https://www.ursi.org/proceedings/procGA05/pdf/F01P.7\(01729\), 2005](https://www.ursi.org/proceedings/procGA05/pdf/F01P.7(01729), 2005)
4. Twati MO, Badi MM, Adam AF, "Analysis of Rain Effects on Free Space Optics Based on Data Measured in the Libyan Climate" in International Journal of Information and Electronics Engineering, 4(6):469-472, 2014
5. Rashidi FU, Semakuwa SK, "Analysis of Rain Effect in Free Space Optical Communication under NRZ Modulation in Two Regions of Tanzania in International Journal of Advanced Engineering and Nano Technology, 1(10):13-16, 2014
6. Singh H, Mittal N. "Performance Analysis of Free Space Optical Communication System Under Rain Weather Conditions" A Case Study for Inland and Coastal Locations of India in Optical and Quantum Electronic, <https://doi.org/10.1007/s11082-021-02848-5>, 2021
7. Chimebuka NJ, "Study on The Effect of Rain on Performance of Free Space Optical Communication". Project Report for the Award of Bachelor In Engineering. Federal University of Technology, Akure. Electrical and Electronics Engineering, 2018
8. Singal P, Rai S, Punia R, Kashyap D. "Comparison of Different Transmitters Using 1550 nm And 10000 nm in FSO Communication Systems, in International Journal of Computer Science & Information Technology, 7(3):107-113, 2015
9. Hameed N, Jatoi TM, Manzoor HU. "Effect of Weather Conditions on FSO link based in Islamabad". Retrieved from <https://arxiv.org>pdf>, 2017
10. Das.N, "Optical communication Systems. Published by InTech, Janeza Trdine 9, 51000 Rijeka", Retrieved from Croatia. <https://www.intechopen.com/books/1339>, 2012
11. Suriza.AZ, Islam MR, Wajdi AK, Naji AW. "Analysis of Rain Effects on Terrestrial Free Space Optical Baswd on Data Measured in Tropical Climate" in IIUM Engineering Journal, 12(5):45-51, 2011
12. Mazin AA. "Atmospheric Turbulence Effect on Free Space Optical Communication, in International Journal of Emerging Technologies in Computational and Applied Sciences, 5(4):345-351, 2013
13. Canuet L. "Atmospheric turbulence profile modeling for satellite-ground laser communication" in MSc. Thesis. Catalonia Polytechnic University. Aerospace Science and Technology Department, 2014

14. Tyagi A, Fajr F, Kumar A, Kaur S. “Proceedings of the International Conference on Innovative Computing & Communications (ICICC) 2020”. Available at <http://dx.doi.org/10.2139/ssrn.3565259>, 2020
15. Andrews LC, Phillips RL. “Laser Beam Propagation Through Random Media” in Bellingham, Washington USA, Spie Press, 2005
16. Sadot.D, Kopelka NS, “Forecasting optical turbulence strength on the basis of macroscale meteorology and aerosols: models and validation” in *Optical Engineering*, 31 (2):200-212, 1992
17. Krishnan P. “Performance Analysis of FSO Systems over Atmospheric Turbulence Channel for Indian Weather Conditions”, in DOI: 10.5772/intechopen.80275, 2019
18. Fadhil HA, Amphawan A, Shamsuddin HAB, Abd TH, Al-khafaji HMR, Aljunid SA, Ahmed N, :Optimization of free space optics parameters: An optimum solution for bad weather conditions”, in *Optic* 124(19):3969-3973. Retrieved from <http://dx.doi.org/10.1016/j.ijleo.2012.11.059>, 2013
19. Maurya V. “Design and Performance Analysis of Visible Light Communication System with Noise Mitigation” in. MSc. Thesis. Malaviya National Institute of Technology, Jaipur. Electronics & Communication Engineering Department, 2019
20. oyoshima M, Takenaka H, Takayama Y. “Atmospheric turbulence-induced fading channel model for space-to-ground laser communications links”in *Optics Express*, 19(17):15965-15975, 2011